

NOTES AND CORRESPONDENCE

The Momentum Imbalance Paradox Revisited

DORON NOF

*Department of Oceanography, The Florida State University, Tallahassee, Florida**

(Manuscript received 1 June 2004, in final form 28 February 2005)

ABSTRACT

The classical problem of a point source situated along a southern boundary emptying buoyant water into a (β plane) ocean is revisited. Pichevin and Nof (PN) have shown that, in contrast to the view prevailing at the time, such an inviscid outflow does not simply turn to the right. Rather, it bifurcates into two branches: a steady branch that does turn to the right (eastward) and an unsteady branch that periodically sheds eddies to the left (westward). This partition is because a simple turn to the right of the entire outflow leaves the outflow's long-shore momentum flux unbalanced, creating a paradox. In contrast, the branching allows the westward-drifting eddies (westward branch) to balance the momentum flux of the steady current (eastward branch). Although the analytical PN solution is useful and informative, it is cumbersome and difficult to apply to actual outflows. Here, a considerably simpler nonlinear analytical solution is presented. Using the idea that the eddies grow slowly relative to their rotation rate, it is shown that an intense (i.e., large Rossby number) and large relative vorticity outflow dumps most of its mass flux (Q) into the eddies (66%). (The remaining 33% goes into the eastward long-shore current.) By contrast, a weak outflow (i.e., an outflow with weak anticyclonic vorticity $-\alpha f$, where α is analogous to the Rossby number and is much smaller than unity and f is the Coriolis parameter) dumps most of its water into the downstream current $[(1-2\alpha)Q]$. Unexpectedly, this partition of mass turns out to be the same as the one taking place on an f plane. (Note that this is not at all the case for southward outflow nor is it the case for either eastward or westward outflow, where β alters the balance drastically.) Although the above partition of mass is independent of β , the size of the eddies generated by the above process is a function of β . It is given by $[768g'Q/\beta\pi f^2\alpha(2-\alpha)(1+2\alpha)]^{1/5}$, where g' is the reduced gravity. This gives a reasonable estimate for the Loop Current eddies' size and generation frequency. Numerical simulations are in agreement with the above nonlinear solution, though the agreement is not necessarily any better than that of PN.

1. Introduction

The problem of how anomalous waters spread once they are dumped into the ocean has been dealt with for decades. The difficulty in solving this problem (of a point source situated along an oceanic boundary) is due to the nonlinearity resulting from the front (i.e., a curve along which the interface, bounding the light water from below, strikes the surface). This front implies that

the variations in thickness are of order unity. The problem is further complicated by the fact that the outflow-generated Rossby waves and Kelvin waves do not necessarily propagate in the same direction. For instance, a northward outflow (our focus here) corresponds to Rossby waves going to the left (looking downstream) and Kelvin waves propagating to the right. By contrast, a southward outflow corresponds to both waves propagating to the right.

Small outflows from rivers or narrow straits (which are not the focus here) are usually governed by frictional and diffusive processes associated with the front. By contrast, large outflows such as that from the Yucatan Strait (which is of interest here) are primarily inertial (inviscid) and nondiffusive. They can be subject to both f and β . On a nonrotating plane (i.e., no Coriolis, no vorticity) such large outflows spread uniformly in

* Additional affiliation: The Geophysical Fluid Dynamics Institute, The Florida State University, Tallahassee, Florida.

Corresponding author address: Prof. Doron Nof, Department of Oceanography 4320, The Florida State University, Tallahassee, FL 32306-4320.
E-mail: nof@ocean.fsu.edu

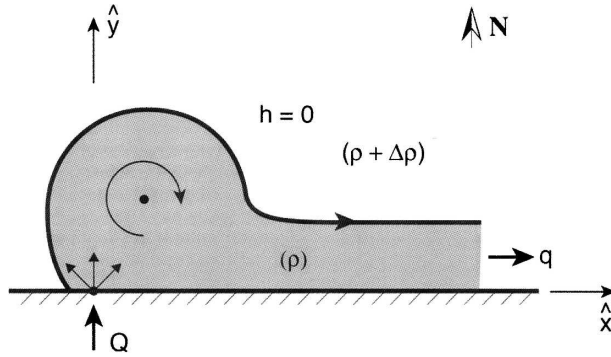


FIG. 1. A schematic diagram of the hypothetical steady configuration shown by Pichevin and Nof (1997) to be impossible on both an f and β plane. In the PN scenario, a steady inviscid outflow cannot exist because the long-shore momentum flux of the downstream current is not balanced. As a result, there are two possibilities. On an f plane, the eddy grows forever and the downstream current mass flux (q) is smaller than the incoming mass flux (Q). On a β plane, the eddy growth is ultimately arrested and, as a result, eddies are periodically shed on the left-hand side (Fig. 2).

all directions. The solution for this problem is simply the potential flow solution (for a point source), which has been known for many years.

By contrast, on an f plane, the problem is already quite complicated. One intuitively expects that, on an f plane, such an outflow would turn to the right in the Northern Hemisphere (because this is the direction in which Kelvin waves go) and form a steady long-shore current. It turns out that this situation is impossible because the momentum flux of the downstream current is not balanced (Fig. 1). To compensate for this downstream flux, a forever-growing eddy is developed next to the source (see, e.g., Nof and Pichevin 2001, hereinafter NP; Pichevin and Nof 1997, hereinafter PN). The growing eddy produces an integrated Coriolis force (in the long-shore direction), which balances the downstream momentum flux. An exception to this point source scenario is that of an outflow from a slanted channel nearly parallel to the coastline. In this case, no eddy is established because the downstream momentum flux is balanced by the upstream momentum flux (in the channel), which is oriented almost in the same sense as the downstream flow (Garvine 2001).

Even though the f -plane problem obviously does not involve Rossby waves propagating in different directions to that of the Kelvin waves, the problem already involves a partition of mass. Using the slowly varying approach, NP showed that $2\alpha Q/(1 + 2\alpha)$ (where Q is the source mass flux and α is the vorticity nondimensionalized by f) goes to the gyre and the remainder goes to the downstream current. Hence, high-vorticity outflows dump most of their water into the eddy, whereas

low-vorticity outflows dump most of their water into the downstream current.

On a β plane, the growing eddy is affected by the tendency of objects to drift to the west. This tendency increases as time goes by because the westward drift is proportional to the eddy maximum thickness (e.g., Nof 1981), which grows in time. There are four possible scenarios where this comes into play. A northward outflow (our focus here), which bifurcates into a steady eastward current and a chain of westward-propagating eddies; an eastward outflow, which produces a steady eddy because the growth is arrested by β (Nof and Pichevin 1999); a southward outflow, which produces a temporary eddy and a broad, westward current in its wake (Nof et al. 2004); and a westward outflow, which also bifurcates into two branches (Nof et al. 2002). In the latter case (westward outflow), the β -plane mass partition is fixed and is independent of the vorticity. Specifically, 7/8 of the incoming transport goes into the coastal current and the remaining 1/8 is going into the eddies. By contrast, on an f plane the partition is heavily dependent on the vorticity. The reader is referred to the above-mentioned references and in particular to Nof et al. (2004) for a description and discussion (see their Fig. 1, p. 794).

Here, we shall focus on the northward-outflow case. This is the first case that we originally investigated (PN) and, ironically, it is one of the most complicated ones. Because of β , the growing eddy ultimately reaches a size where the westward speed is greater than its growth rate. At that point the eddy begins to detach. This process is repeated and, consequently, a branch consisting of a chain of westward-propagating eddies is established (Fig. 2). By integrating the momentum equations over the eddy generation period, PN derived an analytical solution for the problem. Although it is informative, it is cumbersome and difficult to use. Here, we present a much simpler analytical solution based on the slowly varying approach. This approximation was not made in PN because we did not realize at the time that it could be used for this problem. We shall see that the new solution is easier to understand and is easier to use though it is not necessarily in a better agreement with either the numerics or the observations.

Surprisingly, this new solution shows that, to first order, β does not affect the *partition of mass* between the eddies and the downstream current. The partition is the same as the f -plane partition mentioned above (NP). The term “surprisingly” is used above because in all of the other outflow problems (i.e., westward outflow; Nof et al. 2002; southward outflows, Nof et al. 2004; eastward outflows, Nof and Pichevin 1999), β does alter the long-shore momentum balance and, hence, has a major

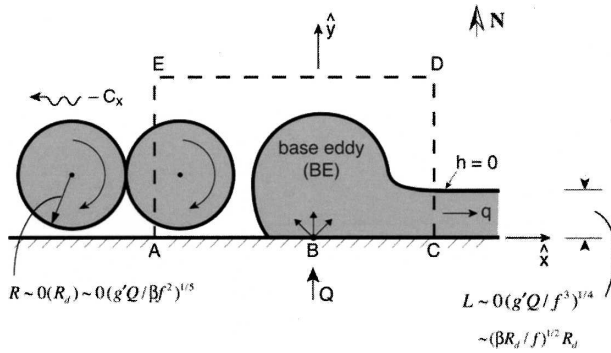


FIG. 2. Schematic diagram showing the PN resolution of the momentum imbalance paradox. “Wiggly” arrow denotes migration. Because of the imbalance shown in Fig. 1, anticyclonic eddies are generated on the left-hand side (looking offshore). Through the β effect, these eddies are forced to propagate to the left. Pichevin and Nof (1997) obtained their analytical solution by equating the momentum flux through EA to the momentum flux through CD. Here, we shall not deal with the momentum flux through EA. Instead, the integrated Coriolis force associated with the slowly growing base eddy (BE) whose center migrates slowly offshore is equated to the momentum flux through CD. The base eddy, which is the eddy in contact with the source, should be distinguished from the already detached eddies downstream. The assumption that the eddies are “kissing” each other as they propagate westward is made in both PN and the present study; \hat{x} and \hat{y} are the fixed coordinates (to be distinguished from x and y , which will later denote the migrating system).

influence on the partition. Specifically, it turns out that, due to β , there is no partition at all in both the southward and eastward cases (i.e., β cancels the f -plane induced partition). In the westward case, on the other hand, 7/8 of the outflow mass flux goes to the eddies and 1/8 goes to the downstream current (regardless of the outflow vorticity).

The paper is organized as follows. Our approach is presented in section 2, the formulation in section 3, the solution in section 4, and the numerics in section 5. The results are summarized in section 6. There is some limited overlap between the present article and both PN and NP because an attempt has been made to make the present paper self-contained.

2. Approach

The geometry is shown in Fig. 3a. As in the f -plane problem (NP), our approach is to look at the “base eddy” (BE) growth process as a slowly varying problem. (By “base eddy” we mean here the eddy that is still in contact with the outflow. It should be distinguished from the already detached eddies farther downstream.) This slowly varying approach is based on the idea that the process involves two time scales, one fast and one

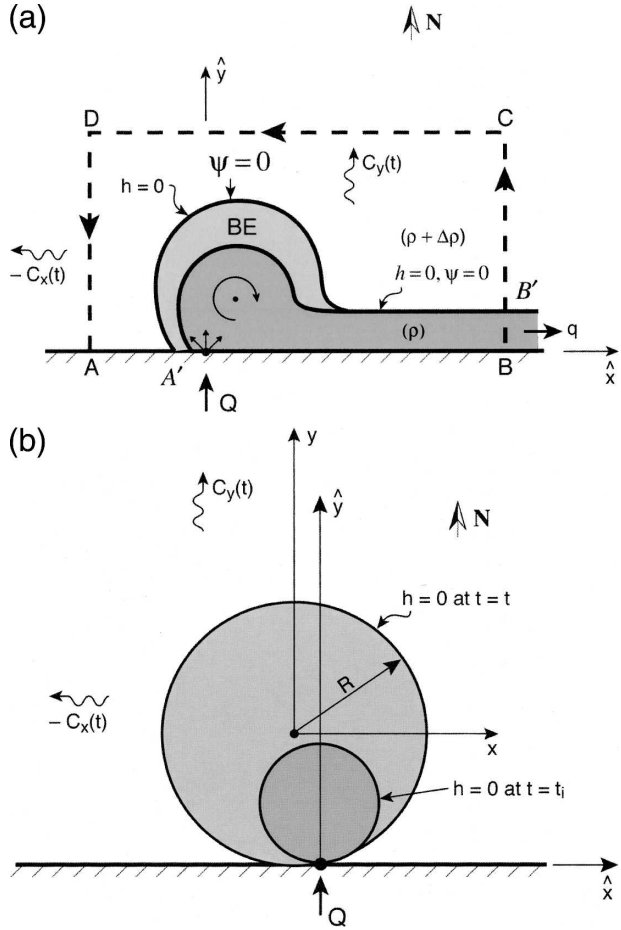


FIG. 3. (a) A schematic diagram of the model under study. As before, the “wiggly” arrow indicates the migration of the BE; it results from both the growth of the base eddy (which forces itself northward, away from the wall) and from β , which forces it westward. This implies that the migration $C_y(t)$ is primarily due to the growth, whereas $C_x(t)$ is primarily due to β . The thick dashed line indicates the integration path that will be used. We focus on “long” time $O(\beta R_d)^{-1}$ so that the process is slowly varying in time. The (immiscible) layers’ densities are ρ and $(\rho + \Delta\rho)$. (b) The approximate structure of the base eddy (i.e., the eddy adjacent to the source). This is the axisymmetric state around which the (slowly varying) perturbation scheme is constructed. At both the initial and consecutive times (t_i and t) the eddy is circular and is barely touching the wall. Note that $C_y(t)$ is mainly due to the eddy’s growth [i.e., $C_y(t) = dR/dt$] whereas $C_x(t)$ is mainly due to the westward motion associated with β . As mentioned, x and y denote the fixed coordinates system whereas \hat{x} and \hat{y} denote the coordinates system moving with the eddy.

slow. The fast time scale [$O(f^{-1})$, where f is the Coriolis parameter] is associated with the time required for a particle to complete a single revolution within the eddy whereas the slow time scale is the time associated with the eddy generation period, $(\beta R_d)^{-1}$, where R_d is the BE Rossby radius. (Note that, for convenience, variables are defined both in the text and in the appendix.)

An outflow that conserves its zero potential vorticity (PV) on both the short and the long time scales will be considered first. That is, we shall initially look at the case where the zero PV is not only conserved at each moment but is also conserved over a long time. It will then become apparent that our slowly varying approach also allows for outflows whose PV is slowly altered in time. This is because, just as the time derivative of the velocity and thickness are negligible (because they vary on the long time scale), so are the small frictional forces which causes the changes in the PV. In addition to the slowly varying approximation (which allows the neglect of all derivatives with respect to time in the governing equations), we shall also construct a perturbation scheme where the basic, undisturbed eddy is a circular eddy “kissing” the wall (Fig. 3b).

Our initial focus on a zero PV outflow is in part unavoidable because the only simple analytical solution for a lenslike eddy on an f plane is the one for a zero PV eddy. We shall later construct analytical solutions for eddies with constant (relative) anticyclonic vorticity smaller than f (corresponding to nonuniform PV). The question of what happens when the incoming fluid has cyclonic rather than anticyclonic vorticity is not addressed here and is left as a subject of future investigation (but see Nof and Pichevin 1999). Note that, strictly speaking, any (inviscid) finite PV outflow has a maximum eddy depth. However, our PV will be allowed to be gradually altered (via small frictional effects) so that such a limit will not exist in our case.

As in NP, we consider the inviscid shallow water equations in a coordinate system traveling slowly with the eddy’s center (section 3). We then consider the integrated balance of forces along the wall and neglect all terms of high order. Ultimately, we find a very simple analytical solution for the base eddy’s increase in size (section 4). It shows that the growth corresponds to a balance between the (long wall) momentum flux associated with the downstream current and the compensating Coriolis force associated with the migration of the base eddy’s center away from the wall.

We shall see that, in this particular case of a northward outflow, β does not enter the zonal long-shore momentum balance so that the partition of mass between the growing eddy and the downstream current is the same as the partition in the f -plane problem. This could not have been anticipated as β *does enter* the long-shore momentum balance in all of the other three cases (westward, eastward and southward outflows). The problem is then closed by assuming that the final detached eddies “kiss” each other as they propagate westward. There is really no physical reason for this to be the case and the condition should be merely viewed

as a closure condition. We shall see later that it corresponds to a *lower* bound on the eddy size.

A numerical “reduced gravity” model (of the Bleck and Boudra type) is then used to show (section 5) that, as the analytical solution predicts, the eddy’s radius increases gradually and that the eddies are periodically shed. We then extend our analytical theory to the cases where the eddy’s relative vorticity is reduced by friction to values much smaller than f . The associated numerical simulations are also in good agreement with this solution. They show that, even though the small frictional effects accumulate over time to alter the PV, the inviscid solution is valid *at each moment*. Application of the theory to the Gulf of Mexico is discussed and the results are summarized in section 6.

3. Formulation

The formulation follows that of NP very closely except that it now includes β corresponding to a Coriolis parameter varying *across* the eddy and downstream current. For clarity, the solution is presented in two stages. First, using the slowly varying approach, all derivatives with respect to time are set to zero. A streamfunction and a perturbation scheme, where the zeroth-order state is a radially symmetric f -plane eddy, are then introduced.

As in NP, the reader is warned in advance that it may be difficult to follow the mathematical analysis in detail. To alleviate some of this difficulty, it is useful to introduce a priori the governing equations that we are after. We shall derive two conservation relationships. The first is the (straightforward) integrated conservation of mass, $dV/dt = Q - q$, where $V(t)$ is the base eddy’s volume (slowly varying in time), Q is the steady outflow’s mass flux, and q is the mass flux of the downstream current. As before, the term base eddy (BE) is used here to indicate the slowly growing eddy attached to the outflow. It is to be distinguished from the already detached eddies, which propagate westward downstream. The second relationship that we seek is the not-so-simple conservation of long-wall (i.e., zonal) momentum flux (or flow force),

$$\iint_S C_y f_\delta h \, dx \, dy = \int_B^C hu^2 \, dy,$$

where S is the base eddy’s area, C_y is the (slow) off-shore migration of the base eddy’s center (i.e., the point of maximum thickness), h is the thickness, and u is the downstream current speed (Fig. 3). Unexpectedly, it turns out that, to the first order, β does not enter this particular balance even though it does enter the long-

shore momentum balance of all of the other cases of outflows on a β plane. Specifically, it enters the balance of a southward outflow (Nof et al. 2004) as well as the westward (Nof et al. 2002) and eastward outflows (Nof and Pichevin 1999). We shall see that the absence of β from our present balance is due to the relatively small scale of the downstream current (as well as the orientation of the coastline). Note that in the analogous problem of a southward outflow (Nof et al. 2004), the outflow develops a larger scale current downstream, allowing a balance between the jet force and a β force (which replaces the migratory term on the left hand in the above relationship).

As in the f -plane case, the term on the left is the long-wall Coriolis force created by the off-wall migration of the base eddy's center (Fig. 3b) resulting from the base eddy's growth (which forces it to push itself away from the wall). The term on the right is the momentum flux of the downstream flow (i.e., the force created by the ejection of mass from the control volume). With the above presentation of the main governing equations, the reader who is primarily interested in the results can now go directly to the solution (4.6)–(4.10).

a. Scales

The “fast” time scale is associated with the (geostrophic) adjustment time scale and with the relatively short time that it takes a particle to complete a single revolution within the (zero PV) base eddy. This fast time [$O(f^{-1})$] is also the time that it takes a particle to get from the base eddy to the downstream current. By contrast, the “slow” time scale [$O(\beta R_d)^{-1}$] is associated with the slow offshore migration of the BE center [$O(\beta R_d^2)$], where R_d is the, yet unknown, eddy Rossby radius that needs to be distinguished from the much smaller downstream current Rossby radius (which is known in advance).

Even though the BE size is not known a priori, it is much easier to initially express the problem scales in terms of the eddy variables. The conceptual small parameter of our problem, $\beta R_d/f$, is the ratio between the short and long time scales or, equivalently, the ratio between the downstream mass flux q (or the incoming mass flux Q , which is of the same order) and the mass flux circulating within the base eddy. To see this more clearly, we note that the volume of the BE at any arbitrarily long time $T \sim O(\beta R_d)^{-1}$ is large [$\sim O(QT)$] because it accumulates mass over the long time period. Since the orbital time is $O(f^{-1})$, the mass flux circulating within the BE [$\sim O(QTf)$] is also large. Furthermore, since the volume of the BE is proportional to the fourth power of the eddy radius (radius square times

the depth which is also proportional to the square of the radius), the radius is large and is given by $\sim O(g'QT)^{1/4}/f^{1/2}$.

Taking H to be the BE maximum depth and h to be the downstream current depth, we immediately see (via geostrophy and the BE/downstream current mass flux ratio) that $h \sim O(\epsilon^{1/2}H)$, where $\epsilon = (\beta R_d/f_0)$ and $R_d = (g'H)^{1/2}/f$. Noting that, via Bernoulli, the speed of the eddy along its edge ($fR/2$) must be equal to the speed of the current along the edge, and taking again into account the current/eddy mass flux ratio ϵ , as well as the downstream current depth scale $\epsilon^{1/2}H$, we find that the downstream current width L is $\sim O(\epsilon^{1/2}R_d)$, implying that the current is narrow relative to the eddy.

In terms of the BE variables, the downstream speed, thickness and width are then fR_d , $H(\beta R_d/f)^{1/2}$, and $R_d(\beta R_d/f)^{1/2}$; the remaining scales are $C_y \sim C_x \sim O(\beta R_d^2)$. As mentioned, the downstream speed is notably large ($fR/2$) because Bernoulli's application to the front ($h = 0$) shows that the speeds of the eddy and downstream current must be the same. This speed is approximately uniform across the narrow downstream current because, even for the zero potential vorticity case, the speed across the current can vary by no more than fL (where L is the current width), which is much smaller than the speed along the edge $fR/2$. It is a simple matter now to connect the unknown eddy variables to the known variables Q , g' , and f . This can be done via the downstream near wall thickness, which via geostrophy, gives $H(\beta R_d/f)^{1/2} \sim (fQ/g')^{1/2}$. It implies that $R_d \sim O(g'Q/\beta f^2)^{1/5}$. Note that, with these scalings, the near wall depth of the downstream current (and, hence, the transport) is independent of β but this is camouflaged by our choice to express all the downstream variables in terms of the BE variables which do depend on β .

We shall now consider the detailed conservation of mass and momentum for the problem. We shall neglect all the time-dependent terms in the (differential) momentum and continuity equations a priori and, once the solution is obtained, show that they are indeed small and negligible relative to the smallest terms that were kept.

b. Mass conservation

The integrated mass conservation equation is

$$\frac{d}{dt} \int_s \int h \, dx \, dy = Q - q, \quad (3.1)$$

where the left-hand side is the slow eddy's volume rate of change and the right-hand side is the difference be-

tween the steady incoming mass flux Q and the outgoing transport of the long-shore current q . Note that the variables x , y , and t are measured in a coordinates system moving with the base eddy's center. They should be distinguished from \hat{x} , \hat{y} , and \hat{t} , which are the variables in the fixed system. The relationships between the two are $x = \hat{x} - \int_0^t C_x dt$, $y = \hat{y} - \int_0^t C_y dt$, and $t = \hat{t}$.

c. Momentum flux

The nonlinear momentum equations (multiplied by h) and the continuity equation are now written in a coordinates system (x, y, t) moving with the eddy's center away from the wall:

$$h \frac{\partial u}{\partial t} + h \frac{\partial C_x}{\partial t} + hu \frac{\partial u}{\partial x} + hV \frac{\partial u}{\partial y} - f(v + C_y)h + \frac{g'}{2} \frac{\partial}{\partial x} (h^2) = 0, \quad (3.2a)$$

$$h \frac{\partial v}{\partial t} + h \frac{\partial C_y}{\partial t} + hu \frac{\partial v}{\partial x} + hv \frac{\partial v}{\partial y} + f(u + C_x)h + \frac{g'}{2} \frac{\partial}{\partial y} (h^2) = 0, \quad \text{and} \quad (3.2b)$$

$$\frac{\partial h}{\partial t} + \frac{\partial}{\partial x} (hu) + \frac{\partial}{\partial y} (hv) = 0, \quad (3.3)$$

where $f = f_0 + \beta\hat{y}$ and, as before, the conventional notation is given in both the text and in the appendix. Namely, u and v are the horizontal velocity components (in the moving coordinate system), C_x and C_y are the time-dependent migration rates in the x and y directions, g' is the reduced gravity, and t is time.

As in NP, the condition $C_y = dR/dt$ (implying that the BE basic state is barely touching the wall at all times) will be used to close the problem (Fig. 3b). The condition is plausible because the BE cannot grow unless it pushes itself away from the wall. Also, we assume that the BE shape is nearly circular at all times. We shall see later that it is clearly supported by the numerics. The x -momentum equation (with β) is now integrated over the area bounded by the thick dashed line shown in Fig. 3a noting that, outside the BE and the downstream current, $h = 0$. With the approximated continuity equation, one finds

$$\iint_s \left[\frac{\partial}{\partial y} (huv) + \frac{\partial}{\partial x} (hu^2) \right] dx dy - \iint_s f(v + C_y)h dx dy + \frac{g'}{2} \iint_s \frac{\partial}{\partial x} (h^2) dx dy = 0. \quad (3.4)$$

We now define the streamfunction ψ to be $\partial\psi/\partial y = -uh$ and $\partial\psi/\partial x = vh$ and rewrite (3.4) as

$$\iint_s \left[\frac{\partial}{\partial y} (huv) + \frac{\partial}{\partial x} (hu^2) \right] dx dy - \iint_s f \frac{\partial\psi}{\partial x} dx dy - \iint_s C_y f h dx dy + \frac{g'}{2} \iint_s \frac{\partial}{\partial x} (h^2) dx dy = 0. \quad (3.5)$$

Application of Green's theorem to (3.5) gives

$$\oint_{\phi} h u v dx - \oint_{\phi} (hu^2 + g'h^2/2 - f\psi) dy + C_y \iint_s f h dx dy = 0, \quad (3.6)$$

where ϕ is the boundary of S (i.e., AA'BB'CDA) and the arrowed circles indicate counterclockwise integration. With the exception of section BB' (Fig. 3a), at least one of the three variables h , u , and v vanish along each section of the boundary ϕ . Namely, $h = 0$ along B'C, CD, DA, and AA' and the meridional speed v is zero along AA'B. Also, with the slowly varying approach, ψ is taken to be a constant along the front ($h = 0$) and is defined to be zero there.

Equation (3.6) can now be written as

$$- \int_B^C \left(hu^2 + \frac{g'h}{2} - f\psi \right) dy + C_y \iint_s h f dx dy = 0, \quad (3.7)$$

where, as before, $f = f_0 + \beta\hat{y}$. As mentioned, application of Bernoulli to the front ($h = 0$) implies that the speed along the outer edge of the downstream current must be approximately equal to the orbital speed along the BE periphery because the pressure is zero in both locations. However, both the thickness and width of the downstream current are small relative to the thickness and radius of the BE. Specifically, within the downstream current u these scales and the zonal orientation of the coastline that filters β out of the problem. Eq. (3.7) can be ultimately written as

$$- \int_B^C hu^2 dy + C_y \iint_s f_0 h dx dy = 0, \quad (3.8)$$

implying that, in sharp contrast to the southward-outflow case (Nof et al. 2004), where the last two parts of the first term in (3.7) are not negligible, and in contrast to both westward outflows (Nof et al. 2002) and eastward outflows (Nof and Pichevin 1999) where β constitutes an additional term, β is not an important part of the present eddy-growing process. As mentioned, this is

because of both the width of the downstream current and the orientation of the coastline.

4. Solution

Having shown that our long-shore momentum balance is identical to that of the f -plane problem because β dropped out of the balance, we can simply write the f -plane solution given by NP for the eddy growth rate (see section 3 in NP). The solution satisfying the initial condition $R_d = R_{di}$ at $t = 0$ is

$$R_d = \left(R_{di}^4 + \frac{g'Qt}{6\pi f^2} \right)^{1/4}. \quad (4.1)$$

Relation (4.1) implies that the instantaneous base eddy's central depth $H(t)$ is

$$H(t) = \left[H_i + Qt \left(\frac{f^2}{6\pi g'} \right) \right]^{1/2}, \quad (4.2)$$

and that the base eddy's radius R is

$$R = \left(R_i^4 + \frac{32g'Qt}{3\pi f^2} \right)^{1/4}, \quad (4.3)$$

where R_i is the initial radius at $t = 0$. The speed that the base eddy's center moves offshore (dR/dt) is

$$C_y = \frac{8g'Q}{3\pi f^2 R^3}. \quad (4.4)$$

As in NP, 2/3 of the outflow's mass flux goes into the eddy and the remaining 1/3 goes into the downstream current. Using our solution (4.1)–(4.4), which is consistent with our initial scaling, it is now a trivial matter to show that all the time-dependent terms originally ignored in our slowly varying derivation (section 3) are indeed small and negligible. [Recall that $C_x \approx C_y \approx 0(\beta R_d^2)$ and $T \sim (\beta R_d)^{-1}$.]

The corresponding expressions for an eddy whose PV is not zero will now be derived. Namely, we shall now consider a BE whose PV is either nonzero to begin with or a BE whose potential vorticity has been very gradually altered (by frictional processes) over a very long period of time. To do this, we consider a BE whose mean (instantaneous) orbital flow (\bar{v}_θ) is given by

$$\bar{v}_\theta = -\frac{\alpha f_0 r}{2}; \alpha \leq 1, \quad (4.5)$$

where r is the radial coordinate.

The BE (instantaneous) volume V is $\alpha(2 - \alpha) \pi f^2 R^4 / 16g'$ and its radius is $R = 2\sqrt{2R_d/\alpha^{1/2}(2 - \alpha)^{1/2}}$. Note that, in general, this BE does not correspond to a uniform PV outflow but all the variables are taken to be of the same order as those of the zero PV eddy. [However,

for $\alpha = 1$, (4.5) reduces to the familiar uniform zero PV case.] Note further that our governing equations are still applicable because, with our perturbation scheme, the downstream current is still narrow relative to the BE and the velocity across it can change by no more than fL . Consequently, the speed of the downstream current ($fR/2$) is taken to be uniform across the current regardless of the BE PV. We find that, as in NP, the ratio of the mass flux going into the growing BE and the incoming mass flux Q is

$$\frac{dV/dt}{Q} = \frac{Q - q}{Q} = \frac{2\alpha}{(1 + 2\alpha)}, \quad (4.6)$$

and that the BE growth rate t is

$$C_y = \frac{dR}{dt} = \frac{8g'Q}{\pi f^2 R^3 (1 + 2\alpha)(2 - \alpha)}. \quad (4.7)$$

At this point, the similarity of our eddy growth β -plane problem to the NP f -plane eddy growth problem ends and we proceed to determine how β does enter the problem. It is argued that it enters the problem only through the slow westward drift of the eddy (which did not enter the momentum and mass balance). This drift ultimately causes detachment. Solving for the detachment process itself is very difficult because of the interaction of the eddy with the wall. To circumvent this difficulty, we now assume (as in PN) that the detached eddies are osculating each other as they move westward and note that the free eddy offshore westward speed (Nof 1981) is

$$C_x = -\frac{\beta R_{df}^2}{3(1 - \alpha/2)} = -\frac{\beta R_f^2 \alpha (2 - \alpha)}{24(1 - \alpha/2)}, \quad (4.8)$$

where R_{df} and R_f are the “final” Rossby radius and radius.

Next, we note that the generation period for each individual eddy (constituting osculating eddies chain downstream) is $2R_f/C_x$, and find that the volume flux going into the eddies (which equals the eddies volume divided by the periodicity) is

$$Q - q = \frac{\alpha(2 - \alpha)\pi f^2 R_f^4}{16g'(2R_f/C_x)} = \frac{\beta f^2 \pi R_f^5 \alpha^2 (2 - \alpha)}{16 \times 24g'}. \quad (4.9)$$

Note that the above free offshore drift speed C_x needs to be distinguished from the forced long-shore drift C_x during the generation process, which cannot be computed with our method because of the unknown pressure field along the wall. Elimination of q between (4.6) and (4.9) gives the final eddy radius R_f ,

$$R_f = \left[\frac{768g'Q}{\beta\pi f^2\alpha(2-\alpha)(1+2\alpha)} \right]^{1/5}. \quad (4.10)$$

As mentioned, the generation period is $2R_f/C_x$ where R_f is now given by (4.10) and C_x by (4.8).

It is important to realize that the kissing condition corresponds to a *minimum* eddy size rather than the maximum size (which our intuition may erroneously suggest). To see this, we denote the separation distance between two consecutive eddies by “ d .” The generation periodicity is now the distance between the eddies’ centers divided by the migration speed $(2R_f + d)/C_x$, and since the mass flux into the eddies is given by $2\alpha Q/(1 + 2\alpha)$, we get

$$\beta\alpha(2-\alpha)(1+2\alpha)\pi f^2 R_f^6 = 24 \times 16g'Q(2R_f + d). \quad (4.11)$$

This relationship shows that a very large value of d (i.e., $d \gg 2R_f$) corresponds to large eddies (i.e., large R_f). It also shows that a minimal d (i.e., $d = 0$) corresponds to the minimal eddy size because the right-hand side of (4.15) is the smallest when $d = 0$. Using (4.11) and (4.10), it is also possible to show that dR_f/dd is *always positive*.

5. Numerical simulations

To examine the validity of our assumptions (e.g., that the flow is parallel to the wall downstream), we shall now present numerical simulations and quantitatively analyze the results.

a. Numerical model description

As in our other outflow problems, we used a modified version of the Bleck and Boudra (1986) reduced gravity isopycnic model with a passive lower layer and employed the Orlanski (1976) second-order radiation conditions for the open boundary. We found that this condition is satisfactory because the downstream streamlines were not disturbed when they crossed the boundary.

We executed several experiments with outflows whose *initial* PV was zero. The results of each experiment within a given group were very similar to each other and, consequently, we present here only four experiments for four different mass fluxes. Because each run provides many data points, it is believed that this presentation is adequate. As is typical for these kinds of experiments, our wall was slippery and the vorticity was taken to be zero next to it. The experiment was begun by turning on an outflow at $t = 0$; the numerical source was a channel containing streamlines parallel to the

channel walls. The initial phase involved the initial establishment of the BE, which could last up to several days.

All of the four runs that we present were conducted with a relatively high resolution corresponding to $\Delta x = \Delta y = 3.6$ km in a basin $360 \text{ km} \times 720 \text{ km}$. For numerical stability, we chose an eddy viscosity of $360 \text{ m}^2 \text{ s}^{-1}$; the time step was 5 min and the upstream thickness along the channel’s right bank was 467 m. Our mass flux was approximately 22, 13, 7, and 3 Sv [where 1 Sverdrup (Sv) $\equiv 10^6 \text{ m}^3 \text{ s}^{-1}$]. We ran all the experiments for a very long time (1000 days) so that the initial potential vorticity was altered by the slow accumulative effects of friction. The above resolution choices were certainly adequate for our Rossby radius of 30 km (corresponding to a g' of $2 \times 10^{-2} \text{ m s}^{-2}$, $f = 10^{-4} \text{ s}^{-1}$, and $H = 467$ m). Furthermore, these choices always allowed for at least 10 grid points across the downstream current, which is also adequate. As in our previous outflow studies, to speed up the experiments and make them more economical, we used a magnified value for β ($10 \times 10^{-11} \text{ m}^{-1} \text{ s}^{-1}$). Also, as in our previous studies, for simplicity, took the speed to be zero along the right upstream channel wall (looking downstream) and the thickness to be zero near the upstream left wall. A zero upper-layer thickness along the left feeding channel wall allows for a faster establishment of the BE because of the elimination of an adjustment near the left corner. Experiments with nonzero values were also conducted but showed very little difference from those shown here.

b. Results

The results are shown in Figs. 4–6 and all show decent agreement with the theory. Fig. 4 shows the bifurcation of the outflow. The eddies appear to be separated from each other rather than kissing each other but this is so because we needed to eliminate the very shallow contours (because of familiar issues with contouring routines). In Fig. 5 we show the mean vorticity in each of the four experiments and the radius of the eddies. Also shown are both the PN values and the present solution values. Note that the PN analytical solution was only given for zero potential vorticity ($\alpha = 1$). For the BE radius our new solution agreement with the theory is slightly better than that of PN. In contrast to this better agreement in radii, the agreement of the transport partition and our new solution is worse than that of PN (see Fig. 6). Nevertheless, our results still are in decent agreement with the numerics. Since the numerical friction reduces the speed downstream and, hence, the downstream jet momentum flux, the required compensating eddies are smaller than the ana-

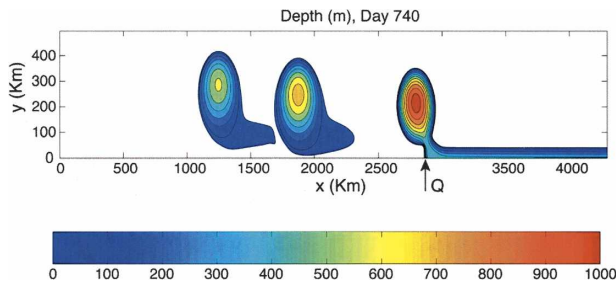


FIG. 4. The results of a typical experiment showing the bifurcation and the establishment of a chain of eddies west of the outflow. Note that the scales on the y and x axes are (intentionally) not the same so that the eddies appear to be slightly elliptical. Also, note that, because of common difficulties with contouring routines, the zero thickness contour ($h = 0$) is not shown (the outermost contour is 20 m) so that the eddies appear to be more separated from each other than they actually are. Physical constants: $f = 10^{-4} \text{ s}^{-1}$; $\beta = 10 \times 10^{-11} \text{ m}^{-1} \text{ s}^{-1}$; $g' = 2 \times 10^{-2} \text{ m s}^{-2}$; $Q = 22 \text{ Sv}$; $R_{do} = 30 \text{ km}$; $R_d = 31 \text{ km}$; $H = 467 \text{ m}$; grid size $\Delta_x = \Delta_y = 5.4 \text{ km}$; time step, $\Delta t = 5 \text{ min}$; eddy viscosity, $500 \text{ m}^2 \text{ s}^{-1}$.

lytics. As a result, the numerical mass flux into the downstream current is *larger* than the analytical flux.

The error introduced by the slowly varying approximation is shown with the shaded regions in Figs. 5 and 6. This error is not that small because we did our runs with values corresponding to the Gulf of Mexico, which is in relatively in low latitude so that the relative variation of the Coriolis parameter with latitude is large. Much of the difference between the analytics and the numerics is due to this aspect. Frictional effects (which, unfortunately, are also not small in the numerics) account for the remaining discrepancy between the analytics and the numerics. These frictional affects are not that small either because the runs lasted for a very long time allowing the frictional contributions to accumulate.

It is appropriate at this point to state the main differences between the PN solution and our new solution. There are four aspects in which the two solutions differ. First, as already alluded to earlier, PN's solution involves the momentum flux of the eddies going out of the control box (Fig. 2) integrated over the period of generation, whereas the present solution involves the integrated Coriolis force associated with the slowly growing BE. Second, the new solution involves the slowly varying approximation (during the eddy generation process), whereas the PN solution does not. Third, PN employed the Bernoulli integral along the southern right wall east of the source whereas the present solution does not invoke such an integration. Fourth, the new solution involves the assumption that the BE is nearly circular whereas the PN solution does not assume anything about the BE. All that it addresses are

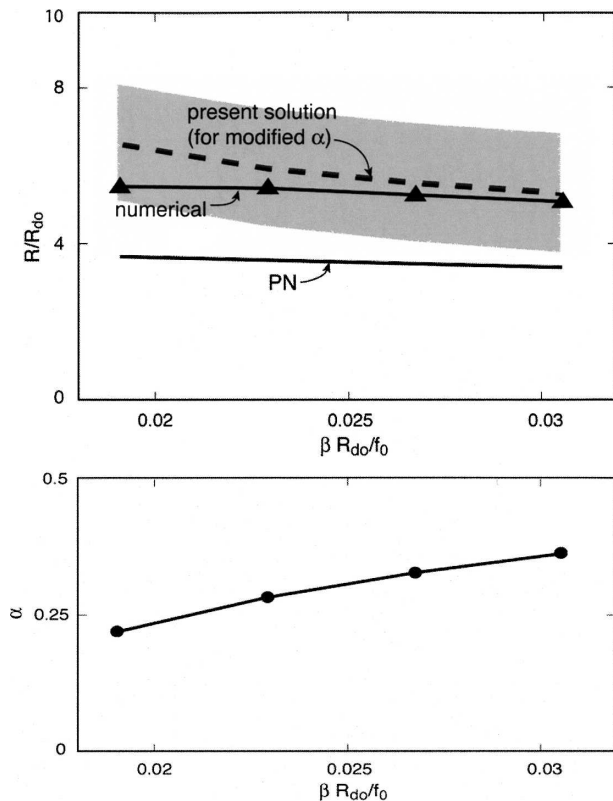


FIG. 5. (top) The analytical solution of PN for the final eddy radius as a function of the outflow's Rossby radius R_{do} [equal to $(2g'Q)^{1/4}/f^{3/4}$] (solid line), the numerical solutions (triangles), and the new analytical solution (dashed line). Note that the new solution is slightly better than the PN solution. The shaded region reflects the error associated with our slowly varying approximation. (bottom) The mean value of α (the ratio between the actual vorticity and f for the core of the eddy where the vorticity is approximately uniform) for each of the four numerical simulations (solid circles). The mean here is the value of α just before the base eddy detachment averaged for four to five eddies generated during each of the experiments.

the detached eddies downstream. (It is for these four reasons that the analytical solution of PN and the present solution compare differently to the numerical experiments.)

Because the PN solution is more complicated than the present one, the only analytical solution that PN gave is that for a zero potential vorticity outflow. (In addition, it should be pointed out that, although PN presented the solution for an outflow associated with a meridional channel, the solution is virtually the same for a point source because neither a channel nor a point source contributes to the long-shore momentum flux.) Last, it is important to realize that our present scales are slightly different from those used in PN. This is so because PN used an integration over the eddy generation period, whereas, here, we merely apply our solu-

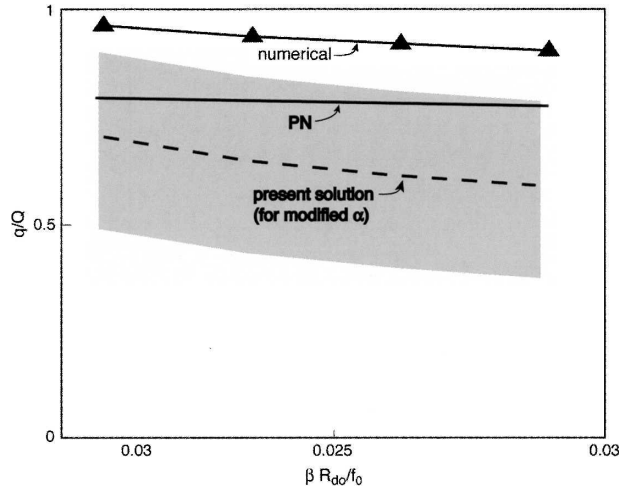


FIG. 6. The same as in Fig. 5 except that we show here the ratio of the mean downstream mass flux q to the incoming mass flux Q . Note that, here, the agreement between the PN solution and the numerics is better than that of the (new) present solution. As expected, the numerics allow more water to go into the downstream current than the analytics because the numerical speeds are reduced by friction. This leads to a smaller momentum flux downstream and, hence, to a smaller compensating mass flux going into the eddies. The shaded area again represents the error introduced by the slowly varying approximation. The remaining differences between the analytical and the numerical values are due to the frictional processes mentioned above.

tion to the long time scale when the eddy is already mature. During the generation period the eddy changes its scale from the relatively small initial outflow Rossby radius R_{do} (the Rossby radius based on Q , g' , and f) to the final large scale that involves β . Similarly, the downstream speed increases as the eddy matures. (Note, however, that the downstream transport is constant, implying that the current thins as the eddy grows.) Because of the changing scales during the eddy generation process, PN had no perfect way to choose the eddy scale and the downstream speed scale. Some sort of an average would have been in order but it is difficult to come up with an appropriate procedure to determine that average. As a “compromise” they took the eddy scale to be the final scale and the downstream speed scale to be the initial speed. Though not perfect, this approach provided reasonable results.

6. Discussion and summary

It was assumed that the eddy nonlinear generation process involves two time scales, a *fast* time scale (i.e., the orbital time scale) and a *slow* time scale (i.e., the time associated with the BE growth and the resulting offshore displacement of its center). Alternatively, the

problem can be thought as involving two speeds, a fast orbital speed (of the fluid within the eddy) and a slow offshore westward migration of the (growing) eddy's center.

The results of the nonlinear theory can be summarized as follows:

- 1) The general analytical solution for the eddy growth (4.6)–(4.7) corresponds to a balance between two long-shore forces, the momentum flux resulting from the downstream current and the integrated Coriolis force resulting from the offshore movement of the base eddy's center (Fig. 3a). Surprisingly, β does not affect the eddy-growth process even though it dramatically alters the growth in the southward-, eastward-, and westward-outflow cases. The nonlinear analytical solution shows that the BE volume, radius, and central depth all gradually increase until the BE is so large that β causes a detachment. Hence, β *does* affect the ultimate eddy size and generation frequency.
- 2) The numerical simulations illustrate that, although the small frictional effects accumulate over time and change the potential vorticity, our most general inviscid solution (4.6)–(4.10) is a valid approximation to the instantaneous structure (Figs. 4–6).

Our results can be applied to various oceanic situations. As pointed out by PN, the flow via the Yucatan Strait can be viewed as an outflow problem. They showed that β is responsible for the ultimate detachment of the rings and calculated their generation periodicity to be roughly 300 days. For consistency, we shall take the same numerical values for the oceanic parameters as those of PN. They are: $g' \approx 1 \times 10^{-2} \text{ m s}^{-2}$, $f \approx 5 \times 10^{-5} \text{ s}^{-1}$, $\beta \approx 2 \times 10^{-11} \text{ s}^{-2} \text{ m}^{-1}$, and $\alpha = 1$. Because of the tendency of nonlinear frontal models such as ours to produce large speeds along the front, PN chose a relatively low value for g' . For the same reason, they also used a relatively low value for the discharge Q and took it to be 20 Sv. For such values the Rossby radius is 42 km. PN's predicted analytical value for the radius of the resulting eddy is 240 km. The corresponding central depth is 640 m, the orbital speed near the edge is 2 m s^{-1} , and the westward drift is 2.1 cm s^{-1} . The generation period was found to be 297 days, very close to the observed values (8–11 months; see e.g., Maul and Vukovich 1993; Sturges 1994). Using (4.10) we now find (with the new solution) the final radius R_f to be 200 km and using (4.8) we find the westward migration speed C_x to be too large, about 6.7 cm s^{-1} . Similarly, the periodicity is disturbingly short, about 70 days. Likewise, for the value of α chosen by PN ($\alpha = 1$), the transport going into the rings is disturbingly large,

about 13 Sv. Luckily, there are very good reasons why these values do not match the actual measurements.

Recent observations (Sheinbaum et al. 2002) published after the publication of PN suggest that PN's choice for the upstream anticyclonic shear (α) is much too high. A value of about 0.2 (instead of the PN value of 1.0) appears to be much more appropriate. With this new value, 29% of the mass flux goes into the rings which are 287 km in radius, drift to the west at a rate of 2.7 cm s^{-1} , have a maximum orbital speed of 1.5 m s^{-1} and are generated every 242 days. With the exception of the orbital speed, which, as is typical for this sort of reduced-gravity model, is high relative to the observed value (50 cm^{-1}), all values are quite reasonable and agree with the mean observed values of 200 km for the radius, 2.9 cm^{-1} for the migration rate, and a generation frequency of 270 days. [see, e.g., Table 2 in Romanou et al. (2004), which provides an excellent summary of all previously observed values]. The analytical orbital speed along the ring rim is high relative to the observed value but this is because in a two-layer model such as ours, the orbital velocity increases monotonically with the radius. [Recall that PN's analytical solution was only derived for the zero PV case ($\alpha = 1$) so we cannot see what a change in α would do to their results.] Note that, in reality, the 29% of the outflow's mass flux that goes into the rings does not disappear from the region because the Gulf of Mexico is closed. A closed basin means that the water that gets into the ring must somehow force other (lower layer) water to find its way out of the basin. Presumably, some of this advected water goes through the deep Yucatan Passage back into the Caribbean but most finds its way into the Florida Current.

It should be noted that, because our model is inviscid, the Froude number along the edge of the coastal current is much larger than unity, suggesting a possible local instability. This is because, along the front, the thickness goes to zero whereas the speed is finite. This is not unusual and is a property of most inviscid coastal currents (see e.g., Stern 1980; Stern et al. 1982). In reality, the Froude number near the front is not large (and, hence, is not unstable) because interfacial friction brings the velocity down (via Ekman layers).

An important question that we left unanswered is how can we a priori determine the vorticity of the eddies. In the large outflows case with an incoming anticyclonic vorticity, such as is the case with the Yucatan Strait, the potential vorticity is conserved and we do not have to worry about this issue. However, in the cases in which the vorticity of the incoming fluid is cyclonic rather than anticyclonic and in the small-outflows case, the fluid must generate an anticyclonic vorticity on its

own (via friction) so that eddies are established. How we can a priori calculate the vorticity that will be generated in these cases is not at all obvious. This is left as a subject for future investigations.

Acknowledgments. The numerical simulations were conducted by Steve Van Gorder. Discussions with W. Sturges regarding the application of the theory to the Gulf of Mexico were very useful. This study was supported by the National Aeronautics and Space Administration Grants NAG5-10860 and NGT5-30513, National Science Foundation Grant 0241036, and Office of Naval Research Grant N00014-01-0291.

APPENDIX

Symbols and Abbreviations

C_x	Long-shore migration of the eddy's center
C_y	Offshore migration of the eddy's center
F	Coriolis parameter
g'	Reduced gravity
H	Eddy's maximum thickness
H	Thickness
L	Downstream current width
Q	Mass flux via the downstream current
Q	Outflow's mass flux
R	Instantaneous eddy's radius
R_d	Rossby radius based on the eddy maximum thickness H
R_{do}	Outflow's Rossby radius; that is, Rossby radius based on the channel near-wall depth
R_{df}	Final eddy Rossby radius
R_f	Final eddy radius
S	Eddy's area
\bar{S}	Area occupied by the basic eddy
t	Time
u, v	Horizontal velocity components
V	Eddy's volume
\bar{v}_θ	Mean orbital flow of an eddy
α	Relative vorticity nondimensionalized with the Coriolis parameter
ϕ	Boundary of eddy's area S
ψ	Streamfunction (defined by $\partial\psi/\partial y = -uh$; $\partial\psi/\partial x = v$)
BE	The base eddy; that is, the eddy that is still in contact with the outflow
NP	Nof and Pichevin (2001)
PN	Pichevin and Nof (1997)
PV	Potential vorticity

REFERENCES

- Bleck, R., and D. Boudra, 1986: Wind-driven spin-up in eddy-resolving ocean models formulated in isopycnic and isobaric coordinates. *J. Geophys. Res.*, **91**, 7611–7621.

- Garvine, R. W., 2001: The impact of model configuration in studies of buoyant coastal discharge. *J. Mar. Res.*, **59**, 193–225.
- Maul, G. A., and F. M. Vukovich, 1993: The relationship between variations in the Gulf of Mexico Loop Current and Straits of Florida volume transport. *J. Phys. Oceanogr.*, **23**, 785–796.
- Nof, D., 1981: On the β -induced movement of isolated baroclinic eddies. *J. Phys. Oceanogr.*, **11**, 1662–1672.
- , and T. Pichevin, 1999: The establishment of the Tsugaru and the Alboran gyres. *J. Phys. Oceanogr.*, **29**, 39–54.
- , and —, 2001: The ballooning of outflows. *J. Phys. Oceanogr.*, **31**, 3045–3058.
- , —, and J. Sprintall, 2002: “Teddies” and the origin of the Leeuwin Current. *J. Phys. Oceanogr.*, **32**, 2571–2588.
- , S. Van Gorder, and T. Pichevin, 2004: A different outflow length scale? *J. Phys. Oceanogr.*, **34**, 793–804.
- Orlanski, I., 1976: A simple boundary condition for unbounded hyperbolic flows. *J. Comput. Phys.*, **21**, 251–269.
- Pichevin, T., and D. Nof, 1997: The momentum imbalance paradox. *Tellus*, **49**, 298–319.
- Romanou, A., E. P. Chassignet, and W. Sturges, 2004: Gulf of Mexico circulation within a high-resolution numerical simulation of the North Atlantic Ocean. *J. Geophys. Res.*, **109**, C01003, doi:10.1029/2003JC001770.
- Sheinbaum, J. J., A. Candela, X. Badan, and J. Ochoa, 2002: Flow structure and transport in the Yucatan Channel. *Geophys. Res. Lett.*, **29**, 1040, doi:10.1029/2001GL013990.
- Stern, M. E., 1980: Geostrophic fronts, bores, breaking and block waves. *J. Fluid Mech.*, **99**, 687–703.
- , J. Whitehead, and B. Hua, 1982: Intrusion of a density current along a coast. *J. Fluid Mech.*, **123**, 237–265.
- Sturges, W., 1994: The frequency of ring separations from the Loop Current. *J. Phys. Oceanogr.*, **24**, 1647–1651.